



New insights into the mucoadhesion of pectins by AFM roughness parameters in combination with SPR

Lars Joergensen^a, Beate Klösken^a, Adam Cohen Simonsen^a, Jonas Borch^b, Ellen Hagesaether^{c,*}

^a Institute of Physics and Chemistry and MEMPHYS – Center for Biomembrane Physics, University of Southern Denmark, Campusvej 55, 5230 Odense M, Denmark

^b Institute for Biochemistry and Molecular Biology, University of Southern Denmark, Campusvej 55, 5230 Odense M, Denmark

^c Institute of Physics and Chemistry, University of Southern Denmark, Campusvej 55, 5230 Odense M, Denmark

ARTICLE INFO

Article history:

Received 23 January 2011

Received in revised form 29 March 2011

Accepted 1 April 2011

Available online 8 April 2011

Keywords:

Mucoadhesion

Pectin

Degree of methoxylation

Amidation

AFM

SPR

ABSTRACT

The object of this study was to assess the mucoadhesion of the three main commercially available types of pectin by atomic force microscopy (AFM) and surface Plasmon resonance (SPR). Polyacrylic acid and polyvinyl pyrrolidone were used as positive and negative control, respectively.

Image analysis of the AFM scans revealed a significant change of roughness parameters when low-ester pectin was introduced to mica supported bovine submaxillary mucin, indicating a high mucoadhesion for this type of pectin. Only minor changes were observed with high-ester and amidated pectin. The same ranking order of adhesion affinity was confirmed by SPR.

In conclusion, a high specific mucin interaction of pectin with a high charge density was demonstrated directly on a molecular scale without interference from the viscoelastic properties or the intra-molecular interactions between the polymer chains themselves, using two independent methods.

© 2011 Elsevier B.V. All rights reserved.

1. Introduction

Mucoadhesive drug formulations are generally considered advantageous, both to prolong the treatment time and the effect of locally acting drugs, but also as a strategy for increasing the bioavailability of elsewhere poorly absorbed drugs, for example proteins and other peptides. In the last case, especially the buccal cavity has emerged as a promising alternative to peroral systemic administration, due to a lower enzymatic activity, a better accessibility and its robustness (Bruschi and de Freitas, 2005). Another advantage of the buccal cavity in the context of exploitation of mucoadhesion is the lower amount of fluid present as compared to for example the gastrointestinal tract. In fact, already in 2005, Rossi et al. published a paper suggesting that buccal drug delivery was a challenge already won. However, even under conditions when the amount of water is rather low, the hydration of a mucoadhesive formulation will increase with time, which will eventually lead to reduced adhesive properties (Surapaneni et al., 2006). When developing a formulation intended to stay on the mucosa for prolonged periods of time, it is therefore of importance to have knowledge about the mucoadhesive properties of polymers in an aqueous environment.

Many different polymers have been synthesized and tested with regard to mucoadhesion (Grabovac et al., 2005). Pectins are cheap, safe and abundant polymers that have been used extensively by the pharmaceutical and food industries (Bengmark, 1998). Commercial pectins consist of a galacturonic acid backbone (Fig. 1). The acid groups can be esterified (methoxylated) or amidated, as indicated by R in the figure. Based on the relative amount of ester groups, pectins are classified into high- and low-ester pectin (HM and LM pectin, respectively). Additionally, LM pectin can be amidated (NH pectin). Due to the manufacturing process, the average molecular weight (Mw) will typically vary between the types. Both the Mw and chemical structure are expected to influence on the mucoadhesion. The mucoadhesive properties of pectins have been investigated by many groups in the past. However, controversial results were reported, and still there is no consensus as to which type of pectin is optimal in view of mucoadhesiveness. LM pectin was reported to be more mucoadhesive than HM pectin for solutions (Schmidgall and Hensel, 2002) and gels (Liu et al., 2005), visualized on porcine colonic tissue and demonstrated by rheological synergism. In contrast, Thirawong et al. found, using a texture analyzer, that HM pectin discs were more mucoadhesive towards a porcine GI mucosa. Amidation had a positive effect on the mucoadhesion of LM pectin (Thirawong et al., 2007). Later they confirmed these findings by rheological synergism studies of pectin solutions and commercially available mucin (Thirawong et al., 2008).

* Corresponding author. Tel.: +45 65 50 35 33; fax: +45 66 15 87 60.
E-mail address: ellen@ifk.sdu.dk (E. Hagesaether).

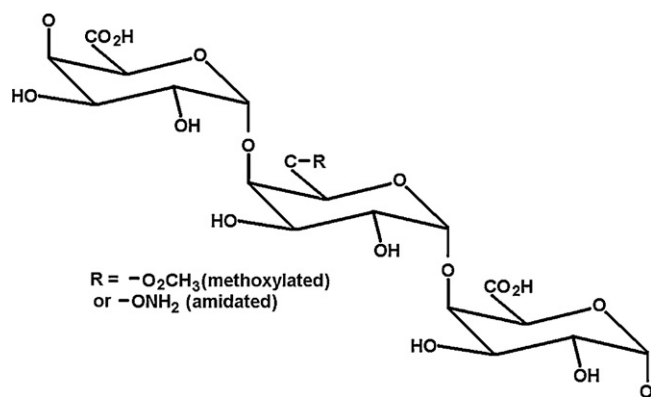


Fig. 1. A schematic illustration showing a part of the galacturonic backbone of pectin, as well as the substitution at the carboxylic acid.

One reason for these conflicting results may be the use of different formulations and methods to test mucoadhesion. Unfortunately, no standardized method exists, and the testing was done in many different ways, ranging from un-physiological *in vitro* situations to *in vivo* testing in animals and humans. Moreover, mucoadhesive interactions have been tested from nanoscale to bulk-level. Advantages and disadvantages exist for all methods. Generally speaking, there seems to be a conflict between gaining information about the important factors and mechanisms involved, and at the same time simulating the relevant *in vivo* conditions.

Atomic Force Microscopy (AFM) is an *in vitro* method that explores the topology and, occasionally, elasticity of a sample in a non-invasive way. A minute tip on a cantilever serves as a nanoscopic finger that probes a sample by scanning it for surface modulations. Essentially, an AFM generates an image that is a 3D map of constant interaction potential between the tip and the surface. The tip-sample interaction is, in a sense, translated into small changes in the bending of the cantilever as it touches or comes close to the sample. The reflection from a laser beam that is incident on the cantilever face can be read on a detector, electronically assembling the image proper from the cantilever deflection. Depending on the AFM settings and the sample details, the resolution for wet samples may go down to the Ångström range, and the images are then depicted on the cm-scale, i.e. in a magnification of $\sim 10^8$.

This setup can allow mucoadhesion to be directly tested on a molecular scale by measuring the force–distance curve between a mucus surface and a polymer microsphere that is attached to an AFM cantilever as a colloidal tip. This approach was successfully used by Cleary et al. to study the molecular interaction between glass beads coated with a co-polymer and bovine submaxillary mucin on a planar carrier, in aqueous surroundings under different pH and salt concentrations (Cleary et al., 2004). Later Catron et al. (2006) did a similar study, but used a sharp AFM tip that was covalently functionalized with polymer molecules to test their affinity for adhering to a mucous interface. However, in Cleary et al.'s self-assessment of their method they point to its complexity regarding functionalization of both the colloidal probe and the planar surface, as well as the effect on reproducibility. This is also indicated by Li et al. (2010) who mostly focused on achieving a smooth and uniform polymer coating of the AFM tip.

The alternative is to focus on topological images that refrain from detailed force measurements, but give an overview of the coverage of a surface with mucin, and on its modification upon interaction with another polymer (Dedinaite et al., 2005). Scans of polymers premixed with mucin have also been used (Deacon et al., 2000). Even this may be a challenge, as getting good and informative pictures of soft matter, especially of swelling polymers in an aqueous environment, is difficult, and there is a risk that the assessment

of the pictures will become somewhat subjective unless a detailed method for the image analysis can be defined.

In this paper we report on a study about the mucoadhesion of pectins, performed by AFM in an aqueous environment cell. We propose to compare and quantify the different interaction behavior found by use of statistical roughness parameters that can be extracted by image analysis from the topographical pictures taken by AFM. Bovine submaxillary mucin (BSM), earlier used to simulate the buccal mucosa, was deposited onto mica and then scanned in air and immersed in water. The pre-coated mica surface was then incubated with different pectin polymers that were introduced into the bulk of the water cell. After washing to remove excessive polymer, AFM images were taken under full hydration. The images obtained were assessed by extracting surface roughness parameters. Their changes depending on the sample details were taken as quantifiers of mucosal adhesion of the polymers under regard. The three main commercially available types of pectin (LM, NH and HM pectin, Table 1) were tested by this method and the outcome was compared to the one obtained for polyacrylic acid (PAA) as a positive control and to the one for polyvinyl pyrrolidone (PVP) as a negative control. PAA and PVP are known to possess high and low mucoadhesion, respectively, e.g. (Thongborisute and Takeuchi, 2008). The results for pectin were validated by an independent method based on surface plasmon resonance (SPR). In short, the change of refractive index upon adhesion of polymer to a test chip is optically explored by the shift of the Plasmon resonance angle in total reflection conditions, which is converted to SPR response measured in resonance units (RU). The SPR response correlates linearly with mass bound to the sensorchip plus the refractive index of the bulk medium (Mol and Fischer, 2010). The test chip consisted of an Au surface that was pre-coated with mucin and mounted into the flow cell of a Biacore instrument. Upon injection of the different polymers into the flow cell, their mucoadhesion was directly monitored. If the polymer permanently binds to the mucinated surface, the refractive index along the sensor chip surface is modified, leading to a quantitative SPR signal in so called response units (RU, in effect proportional to the interfacial refractive index).

2. Materials and methods

2.1. Materials

Mucin from bovine submaxillary glands (BSM), type I–S, batch 068K7001, was purchased from Sigma–Aldrich and used as received.

5 different test polymers were used, all dissolved in pure water. The LM, NH and HM pectin were derived from citrus and kindly provided by the manufacturer (CP Kelco, Denmark) and used as received. Details are listed in Table 1. The pectins differed in the degree of and functionalization (methoxylation and amidation) of the acid groups, as well as Mw. Polyacrylic acid (PAA; Carbopol 980, batch 80035089) and polyvinyl pyrrolidone (PVP; Povidone 25, batch 81430488) were used as positive and negative control, respectively. They were both of Ph. Eur. quality and purchased from Caelo, Hilden, Germany. Both were used as received.

Milli-Q water from a QTUM000EX obtained from Millipore A/S, with a 0.22 μm filter unit on the outlet was used as solvent.

All other chemicals were of analytical grade.

2.2. Methods

2.2.1. Atomic force microscopy (AFM)

AFM was performed with a PicoScan – AFM (PicoSPM from Molecular Imaging Inc. (now Agilent Technologies Inc.)) using a scanner that has a maximal range of 30 $\mu\text{m} \times 30 \mu\text{m}$. Sam-

Table 1
The types of Genu® pectin investigated.

	Low-ester (LM) pectin	Amidated (NH) pectin	High-ester (HM) pectin
Brand ^a	LM-12 CG-Z	LM-102 AS-Z	Type B Rapid Set-Z
Batch ^a	GR84468	S73081	GR82670
Degree of methoxylation ^{a, b}	33%	30%	70%
Degree of amidation ^{a, b}	0%	19%	0%
Intrinsic viscosity ^c , $[\eta]$ (dL/g)	3.35	4.31	5.36
Huggins' constant ^c , k'	0.38	0.37	0.44

^a Information provided by the manufacturer.

^b Amount of substituted sites/amount of monomers $\times 100$ (%).

^c Details about the viscosity measurements can be found elsewhere (Hagesaether, 2011).

ples were deposited onto mica (G250-1 from Plano GmbH, Germany). AFM imaging was done in air in the contact mode (cantilevers by NanosensorsTM, type PPP-NCL-50, $\nu \approx 146$ –236 kHz, $k \approx 21$ –98 N/m) or, alternatively, in a water cell in Mac mode (cantilevers by NanosensorsTM, MAC type PPP-MFMR-20, $\nu \approx 73$ –87 kHz, $k \approx 2.3$ –3.9 N/m) under full hydration. Instrument control and image acquisition was performed using the PicoScan software (v5.3.3). The SPIP software (Image Metrology, V3.3.4.0) was chosen for image processing and analysis.

Samples for AFM were based on an initial coating of mica with BSM. Mucoadhesion was then later explored by doing AFM on pre-coated samples that were incubated in aqueous solutions of a test polymer to be studied for its mucoadhesive properties.

For the coating, mica was cut (size of 80–100 mm²) and freshly cleaved using ordinary scotch tape. At once, 100 μ L of 2.00 wt.% BSM dissolved in 12.5 mM NaCl was applied onto the mica plate. The next day, after evaporation of all solvent, all samples were first scanned in air to confirm similarity among them (scan size: 2.5 μ m \times 2.5 μ m). Then the samples were mounted into a liquid cell and rehydrated with 500 μ L of pure water. These samples were then scanned a total of 7 times with the AFM under wet conditions.

Thereafter, 100 μ L of test polymer was injected. The concentrations used were 0.001 wt.% for pectin, while for the control polymers, PAA and PVP, the concentration was raised to 0.010 wt.% in order to maximize the effect. The samples were incubated for 10 min, followed by repetitive washing ($10 \times \sim 500$ μ L). During this removal and adding, there was always a minimal amount of ~ 100 μ L of water keeping the sample fully wetted and finally leaving it covered with ~ 500 μ L of water. At once, the sample surface was scanned again several places by AFM such as to detect changes in the sample topology that might have arisen from the mucoadhesion of the polymer during the incubation time.

All images were pretreated by plane correction before further analysis. Plane correction was done with SPIP using a histogram alignment on the entire image with an average profile fit as global correction and the z offset method bearing height zero.

Thereafter, standard roughness parameters were extracted from all images, again using SPIP. Areas of odd features were avoided and the remaining image used for calculating the roughness parameters. The roughness parameters are statistical quantities extracted from the topology variation of a (complete) scan image. 2 roughness parameters are considered in this paper. They are both expected to change upon adhesion towards a surface. The root mean square (Sq) of the roughness average (Sa, the average deviation of the local height from the average height) is defined in Eq. (1.1). The peak–peak height (Sy) is the height differences between the highest and lowest peak in the image (Eq. (1.2)).

$$Sq = \sqrt{\frac{1}{NM} \sum_{k=0}^{M-1} \sum_{l=0}^{N-1} (z(x_k, y_l) - \mu)^2} \quad (1.1)$$

$$Sy = z_{\max} - z_{\min} \quad (1.2)$$

2.2.2. Surface plasmon resonance (SPR)

SPR was performed in a Biacore 3000 equipped with BIAevaluation software (GE Healthcare, Uppsala, Sweden) using a bare gold sensorchip (type SCB AU-5, Xantec Bioanalytics GmbH, Düsseldorf, Germany). The microfluidic flow system of the Biacore instrument forms 4 flow cells on the sensorchip that can be addressed individually or in combinations. All samples were filtered through a 0.45 μ m pore filter (Minisart, 16555 80412103) before injection to remove any dust particles or other big sized objects that might interfere with the free flow in the microchannel lines. All liquids used for SPR were degassed before use in order to avoid the development of gas bubbles that can interfere with the flow and detection.

At first a baseline with pure degassed water was established over a course of 3 min. Then the chip was conditioned with BSM dissolved in pure water (0.10 wt.%). Five injections of BSM were applied sequentially, followed by water washing, to condition each of the sub-cells separately, covering the detection surface of the Au chip with a layer of BSM. The final outcome for each of the flow cells was then found in RU units for each of the flow channels on the chip. Finally, test polymer solutions were applied, each in at least 3 subsequent injections to individual BSM coated channels and the specific SPR signals were recorded. LM, NH and HM pectin, as well as the negative control PVP (all provided as 0.10 wt.% in water solution) were tested for binding. All experiments were performed at 25 °C; the flow rate was 15 μ L/min, and the injection time for BSM and the test polymers was 1 min. After each injection, the cell was flushed with water for 4 min.

3. Results and discussion

3.1. AFM

Representative images from the 3 essential preparative steps are shown in Fig. 2. First, the mica carrier was exposed to the BSM solution. After evaporation of the solvent, it was found fully covered with BSM (Fig. 2a)). The lighter areas indicate more concentrated and bulky BSM, while the black areas represent a thinner layer of BSM. The covering is hence not uniform. The BSM samples were rehydrated and then imaged in the wet state in a water cell (Fig. 2b)). The BSM probably swells and hence changes conformation when rehydrated. This gives rise to a different roughness variation, as can be seen by a lot of small blobs and a few big ones (lighter areas) sitting on a background of apparently more homogenous topology. Then, the BSM coating in the water cell was incubated with test polymer by injection of the selected polymer type and, after incubation, the excess polymer was removed by washing. A scan obtained from PAA as test polymer is shown in Fig. 2c). In this case the surface topology appears smoother, indicating that PAA interacted with the BSM surface. Blobs can still be identified. Although, in general, the individual scans reveal an uneven surface containing different features, all samples were considered as macroscopically homogeneous on average. Therefore all scans from the accidentally chosen spots in a sample are represen-

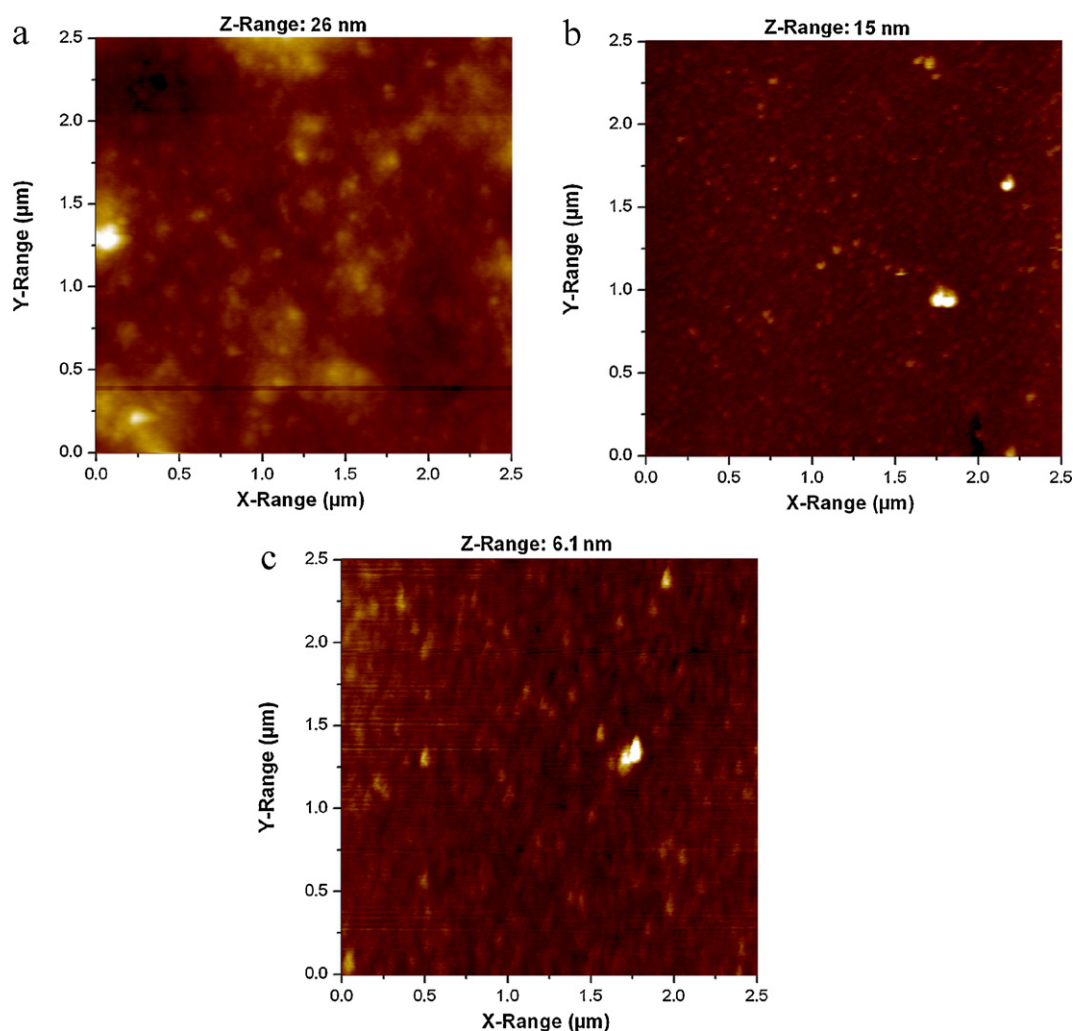


Fig. 2. (a) BSM on a mica sheet, imaged in dry state in ambient air (b) rehydrated BSM on mica, mounted into a water cell (c) rehydrated BSM on mica after incubation with PAA and subsequent washing (imaged under full hydration in water cell).

tative of the sample. It is thus no problem that it is impossible to probe the exact same spot of a sample in the early stages of coating and after further injections.

The images show that BSM and test polymer are deposited onto the carrier sheet. Still, distinct conclusions regarding quantification of adhesion of test polymer to the initial BSM coating can hardly be drawn from the shear appearances of the samples. Only a statistical analysis and subsequent comparison among samples of different preparations does allow a quantification of the mucoadhesive potential of the diverse test polymers.

The selected quantities (see Eqs. (1.1) and (1.2)) from the statistical image analysis are presented graphically in Fig. 3a and b. They compile the results obtained by AFM under hydrated conditions. The initial BSM values (light bars) are an average from all samples and are used as start values which are compared to the properties after application of test polymer (dark bars; averaged as indicated in the figure caption).

The root mean square of the roughness average of BSM was not changed by PVP, serving as the negative control polymer (Fig. 3a)). On the other hand, the positive control polymer PAA reduced the variation of the average roughness drastically, as was also apparent from direct observations (Fig. 2c)). The pectins, at a 10 times lower concentration, displayed intermediate values. Among the pectins, only LM pectin inflicted changes that were statistically significant. The samples were more homogeneously flat over the whole scan

area after application of PAA and LM pectin, indicating an interaction with BSM. In general, the peak–peak height values confirmed this picture (Fig. 3b)).

3.2. Surface plasmon resonance/Biacore

The Biacore method has previously been reviewed as an alternative *in vitro* method to detect the mucoadhesive properties of polymers, and the results obtained corresponded well with the results of other mucoadhesion tests (Takeuchi et al., 2005).

First the Au-surface was covered with BSM. BSM attached very effectively to the surface of gold as demonstrated by the increase in SPR response: the average change relative to the water baseline for the 4 flow cells after five injections was 633 ± 48 (SD) RU. Furthermore, the BSM was attached relatively stably to the Au surface as seen by the slow decrease of SPR response after the flow was changed to water. Next, test polymers were injected in the BSM coated flow cells and the change in SPR response for each individual channel with test polymer was recorded. As an example the result displayed by LM pectin is shown in Fig. 4, as well as an explanation for the Δ RU values. The initial BSM baseline value was set to 0 RU. During the first injection, a large increase in SPR response is obtained. This signal is due to both the adhesion of test polymer (LM pectin) to the BSM matrix on the chip as well as the presence of the test polymer in the bulk solution. After first flushing (\downarrow) with

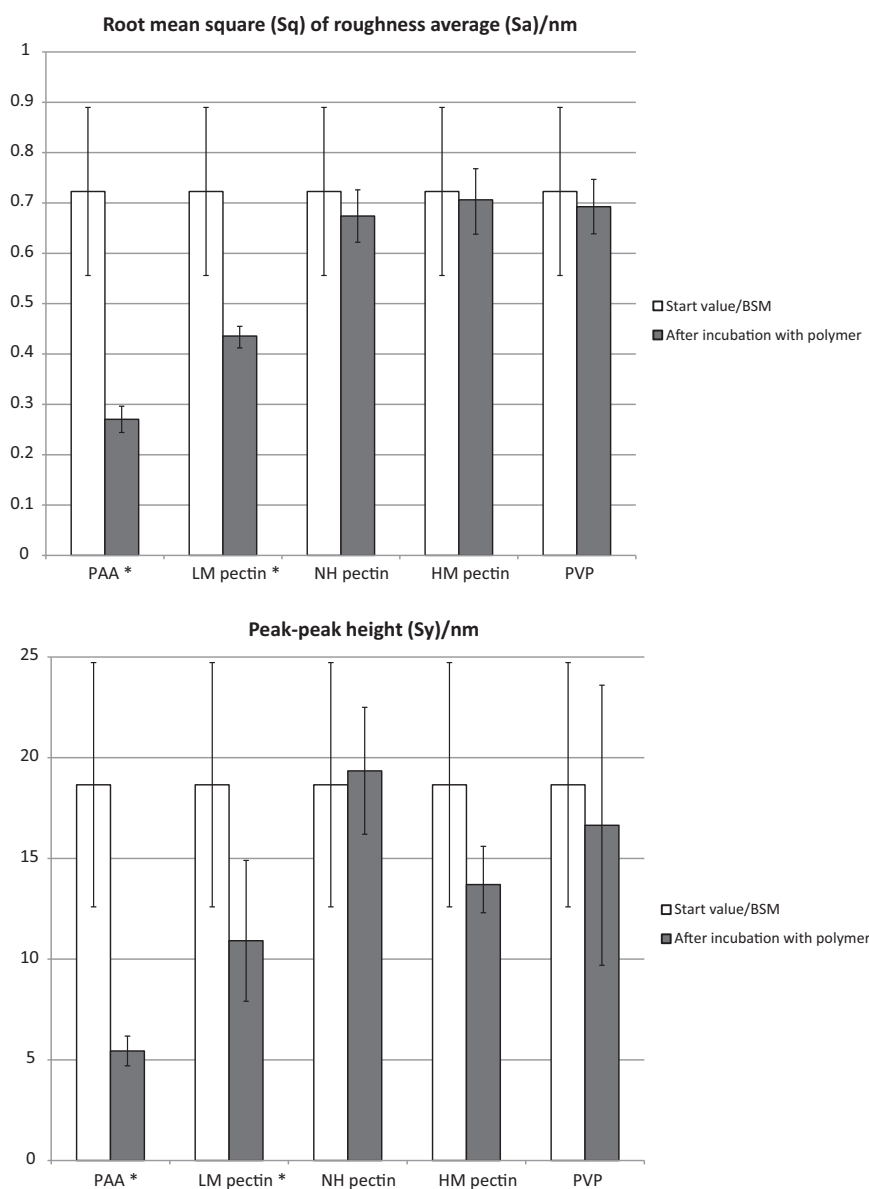


Fig. 3. The selected quantities from the statistical image analyses (a) Root mean square (Sq) of the roughness average (Sa) (b) Peak-peak height (Sy). The results are expressed as the mean with the bar showing the standard deviation for BSM, PAA and PVP and the min and max values for the pectins. The numbers of scans were: $n = 7$ for BSM, $n = 4$ for PAA and PVP, $n = 3$ for LM and HM pectin, $n = 2$ for NH pectin. The values were tested for significant statistical differences ($p < 0.05$) after incubation with polymer. If this was the case, the test polymer is marked with a star (*).

water, the net SPR response that is significant for the adhesion is obtained (injection 1). Further injection (\uparrow) resulted in additional adhesion with declining efficacy, until the surface is saturated. The total increase in net SPR response of all injections after flushing with water can be taken as an indicator of adhesion affinity. The results for all test polymers are compiled into Table 2.

The negative control, PVP, displayed a very low change of SPR response relative to the baseline. This was also the case for NH pectin. LM pectin displayed the largest increase in SPR

response, indicating an accumulation of LM pectin at the BSM interface. The values of HM pectin were in between those of LM and NH pectin. The results from the Biacore method thus correlated well with the observations from AFM: among the pectins, mucoadhesion was highest for LM pectin. Unfortunately, the experiments with PAA using this set-up were unsuccessful due to clogging. A high mucoadhesion for PAA compared to PVP has previously been reported using SPR (Thongborisute and Takeuchi, 2008).

Table 2
Increment in SPR response obtained from the Biacore measurements after injections of test polymers over a BSM covered Au-surface (the explanation for the values is given in Fig. 4).

Δ RU/polymer	LM pectin (Δ RU)	NH pectin (Δ RU)	HM pectin (Δ RU)	PVP (Δ RU)
Injection 1	141.8	8.7	86.6	18.2
Injection 2	49.5	9.9	31.3	11.7
Injection 3	34.5	11.1	16.5	10.9
Sum	225.8	29.7	134.4	40.8

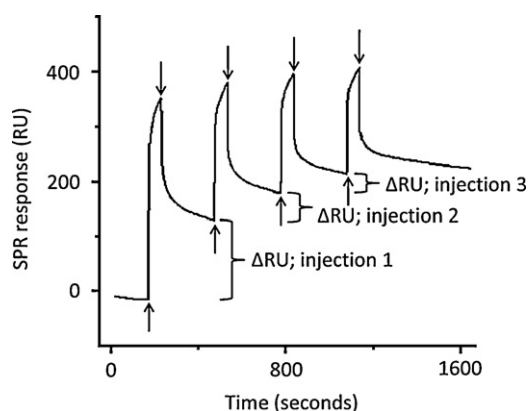


Fig. 4. Sensorgram of the Biacore measurements when LM pectin was injected onto a BSM covered Au-surface (baseline value set to 0 RU). Each injection time point of polymer is indicated by an arrow turning upwards (↑) and flushing is indicated by an arrow turning downwards (↓). Thus there is a constant flow of polymer between sets of upwards and downwards arrows and of water between downwards and upwards arrows.

3.3. General discussion

The different theories and mechanisms behind mucoadhesion have been reviewed many times, e.g. (Smart, 2005). For example, for a dry formulation, mucoadhesion can be viewed as a step-wise process, with a first step consisting of establishing an intimate contact between the mucoadhesive and the mucous membrane, and a second consolidation step, where various molecular interactions of physicochemical nature occur to consolidate and strengthen the adhesive joint. During the first step, at least two processes can occur that may lead to adhesion. One is related to swelling of the formulating, liberating the polymer chains. In this way, the optimum in viscosity at the surface, leading to a general adhesion, tack, may be reached. The other is related to the formulation extracting water from the underlying mucosa, leading to adhesion by capillary attraction or as a result of the increased strength of the mucosa (Marshall et al., 2004). However, as the hydration of the initially dry formulation gradually increases with time, the adhesion established during step one will decline, unless compensated by another mechanism. It is therefore step two that is responsible for prolonged adhesion, which in some cases is beneficial for drug treatment. We therefore decided to focus on step two. This was achieved by studying the molecular interactions between a surface that mimics the buccal mucosa and test polymer solutions of a low concentration. In that way, step one can be disregarded, and it can be assumed that the test polymers are fully hydrated, possess maximum flexibility and minimal intra- and intermolecular bonding, i.e. they are in their most uncoiled configuration.

The test polymers used in this study all possess a different Mw. This is often the case for different types of polymers, especially those of a natural origin. The Mw of a polymer is a parameter that can influence the adhesive properties, in addition to chemical structure. Therefore, assessing the impact of differences in Mw is important. In general, for highly soluble polymers like pectin, a high Mw will increase the viscosity of a polymer solution, leading to a higher tack and hence a general tendency for adherence to most types of surfaces, including those covered by mucus. For the polymers in this study, the positive control, PAA (Carbopol 980) is known to possess a very high Mw of a few million Da, while the negative control, PVP (Povidon 25) has a Mw of about 15–30 kDa. The intrinsic viscosities for the different types of pectin can be seen in Table 1. Using the Mark–Houwinks relationship, $[\eta] = K \times Mw^a$, and the constants for K and a obtained from (Christensen, 1954) or (Anger and Berth, 1986), the Mw can be estimated to vary from

about 70 kDa for LM pectin to about 115–135 kDa for HM pectin, with amidated pectin having a Mw in between. This method has been used previously (Hiorth et al., 2003). The results are reasonable, as the manufacturing process used to produce LM pectin from HM pectin is also known to invoke hydrolysis of the pectin backbone. Either because of this difference in Mw or, alternatively, due to the higher number of hydrophobic groups, 3.0 wt.% solutions of HM pectin generally displayed a higher viscosity and hence a higher tack. This further lead to a higher unspecific adhesion and hence a higher general mucoadhesion than LM pectin (Hagesaether and Sande, 2007). The same effect was observed for casted films (Hagesaether and Sande, 2008).

However, the pectin concentrations used in this study were only 0.001 wt.% during the AFM measurements and 0.1 wt.% during the Biacore measurements. Using the same values for intrinsic viscosity, the concentration when the pectins start to overlap can be calculated to be ca. 0.2 wt.% and hence higher than the concentrations used in this study. Additionally, the differences in viscosity of the pectin solutions are negligible as determined by capillary viscosimetry. In that way, the mucoadhesion of pectins was tested here on a molecular level, without interference from the viscoelastic properties nor the intra-molecular interactions between the polymer chains themselves.

In this study, both the AFM and Biacore measurements indicate that LM pectin was more mucoadhesive than amidated and HM pectin, despite having a lower Mw. Reasons for this can be that LM pectin interpenetrated the mucin network easier or displayed intermolecular interaction with the mucin molecules. This is in line with our earlier studies, where LM pectin showed a particularly strong estimated specific interaction with mucin (i.e. the adhesion remaining after the unspecific adhesion have been mathematically subtracted), which was demonstrated for 3.0 wt.% solutions and casted films by tensile tests (Hagesaether and Sande, 2007, 2008). For solutions, the superior mucoadhesive properties of LM pectin were, by adding urea, demonstrated to be caused by hydrogen-bonding. The importance of hydrogen-bonding in mucoadhesion has been highlighted several times, and the presence of $-COOH$ and $-OH$ groups are generally regarded as beneficial with respect to mucoadhesion. Mucin will be negatively charged at $pH > 3$, and the free carboxylic acid groups of pectin have a pKa of about 3. The fact that both mucin and pectin are negatively charged, and that water itself is a strong hydrogen bonding substance, may make the results and explanation seem paradoxical. However, it has previously been suggested that the electrostatic repulsion with the same charges may cause an uncoiling of polymer chains, which may facilitate chain entanglement and bond formation (Sriamornsak et al., 2010). Even more, some surprising hydrogen-bond attraction forces have been measured between carbohydrates and mucin in solution. This was attributed to matching active site patterns, thereby being able to compete with the strong hydrogen-bonding properties of water (Huang and Peppas, 2007). The negative charges of mucin and pectin make them a stronger electron donor than water, and hydroxyl groups can act as electron acceptors.

Mucoadhesion was found to be low or non-existing for NH pectin for both methods. HM pectin displayed an inconsistent change of AFM roughness parameters, but during the Biacore® experiment, values in-between those displayed by LM and NH pectin were observed. During these experiments, the concentrations were 100 times higher than during AFM. Therefore, despite clear differences in the thermodynamic conditions during the different types of experiments, some contribution from the higher viscosity to the intermediate mucoadhesion observed, cannot be ruled out.

Solutions of mucin, pectins and mixtures of mucin and pectin were scanned with AFM in a recent study (Sriamornsak et al., 2010). From the pictures they concluded that NH pectin is the

most mucoadhesive. They did not consider the change in roughness parameters, which was shown in this study to be useful. In fact, already in 2000 Patel et al. assessed the arithmetic roughness average when testing the mucoadhesion of polycarbophil, chitosan and hydroxypropyl methylcellulose towards a buccal cell surface, and in 2006 Svensson et al. observed a change in roughness of the surface when BSM and chitosan was deposited layer by layer in an AFM liquid cell.

The usefulness of using the change in roughness parameters as an indication of mucoadhesion was indicated by the negative and positive control polymers, PVP and PAA, respectively. PVP displayed insignificant while PAA displayed significant changes. PAA is also a polymer with many acidic groups and hence possesses negative charge in a pure water solution. However, in contrast to pectins, PAA lacks electron acceptors. The influence of the extremely high Mw and viscoelastic properties can therefore not be completely ruled out as an explanation.

In conclusion, the promising mucoadhesion of LM pectin in solution, previously reported by us using estimated specific mucin interaction, was here demonstrated directly on a molecular scale by two independent methods. A high charge density due to free acid groups was found more important for high mucoadhesion than high Mw or amidation. Due to the low concentrations used, neither the viscoelastic properties of pectin solutions nor the intra-molecular interactions between the polymer chains themselves interfered with the results.

SPR and roughness parameters from AFM allowed to explicitly measure the specific mucin interaction, i.e. the second adhesion step, without subtracting the tack and unspecific adhesion. The results for pectin obtained during the AFM experiments were compared to the behavior of PAA as positive and PVP as negative control, respectively. Additionally, the results for pectin generally correlated with those given by an independent method; SPR. The AFM method can therefore be recommended as a starting point when choosing between different mucoadhesive polymers, also for polymers intended for mucoadhesion in the gastrointestinal tract, as the interaction was studied in an aqueous environment.

Acknowledgement

We would like to thank Raúl Hernández Sánchez for help with SPR measurements. The work was supported by a generous grant from the Danish National Research Foundation driving MEMPHYS-Center for Biomembrane Physics.

References

Anger, H., Berth, G., 1986. Gel permeation chromatography and the Mark–Houwink relation for pectins with different degrees of esterification. *Carbohydr. Polym.* 6, 193–202.
 Bengmark, S., 1998. Immunonutrition: role of biosurfactants fiber, and probiotic bacteria. *Nutrition* 14, 585–594.
 Bruschi, M.L., de Freitas, O., 2005. Oral bioadhesive drug delivery systems. *Drug Dev. Ind. Pharm.* 31, 293–310.

Catron, N.D., Lee, H., Messersmith, P.B., 2006. Enhancement of poly(ethylene glycol) mucoadsorption by biomimetic end group functionalization. *Biointerphases* 1, 134–141.
 Christensen, P.E., 1954. Methods of grading pectin in relation to the molecular weight (intrinsic viscosity) of pectin. *J. Food Sci.* 19, 163–171.
 Cleary, J., Bromberg, L., Magner, E., 2004. Adhesion of polyether-modified poly(acrylic acid) to mucin. *Langmuir* 20, 9755–9762.
 Deacon, M.P., McGurk, S., Roberts, C.J., Williams, P.M., Tendler, S.J.B., Davies, M.C., Davis, S.S.B., Harding, S.E., 2000. Atomic force microscopy of gastric mucin and chitosan mucoadhesive systems. *Biochem. J.* 348, 557–563.
 Dedinaite, A., Lundin, M., Macakova, L., Auletta, T., 2005. Mucin–chitosan complexes at the solid–liquid interface: multilayer formation and stability in surfactant solutions. *Langmuir* 21, 9502–9509.
 Grabovac, V., Guggi, D., Bernkop-Schnürch, A., 2005. Comparison of the mucoadhesive properties of various polymers. *Adv. Drug Deliv. Rev.* 57, 1713–1723.
 Hagesaether, E., 2011. Permeation modulating properties of natural polymers – effect of molecular weight and mucus. *Int. J. Pharm.* 409, 150–155.
 Hagesaether, E., Sande, S.A., 2007. In vitro measurements of mucoadhesive properties of 6 types of pectin. *Drug Dev. Ind. Pharm.* 33, 417–425.
 Hagesaether, E., Sande, S.A., 2008. In vitro mucoadhesion of pectin films, effect of type of polymer and plasticizer. *Pharm. Dev. Technol.* 13, 105–114.
 Hiorth, M., Tho, I., Sande, S.A., 2003. The formation and permeability of drugs across free pectin and chitosan films prepared by a spraying method. *Eur. J. Pharm. Biopharm.* 56, 175–181.
 Huang, Y., Peppas, N.A., 2007. Nanoscale analysis of mucus–carrier interactions for improved drug absorption. In: Peppas, N.A., Hilt, J.Z., Thomas, J.B. (Eds.), *Nanotechnology in Therapeutics*. Horizon Bioscience, Wymondham, UK, pp. 109–129.
 Li, D., Yamamoto, H., Takeuchi, H., Kawashima, Y., 2010. A novel method for modifying AFM probe to investigate the interaction between biomaterial polymers (Chitosan-coated PLGA) and mucin film. *Eur. J. Pharm. Biopharm.* 75, 277–283.
 Liu, L., Fishman, M.L., Hicks, K.B., Kende, M., 2005. Interaction of various pectin formulations with porcine colonic tissues. *Biomaterials* 26, 5907–5916.
 Marshall, P., Snaar, J.E.M., Ng, Y.L., Bowtell, R.W., Hampson, F.C., Dettmar, P.W., Onsøyen, E., Melia, C.D., 2004. Localised mapping of water movement and hydration inside a developing bioadhesive bond. *J. Control. Release* 95, 435–446.
 Mol, N.J.d., Fischer, M.J.E., 2010. Surface plasmon resonance: a general introduction. In: Mol, N.J.d., Fischer, M.J.E. (Eds.), *Methods in Molecular Biology*. Humana Press, New York, USA, pp. 1–14.
 Patel, D., Smith, J.R., Smith, A.W., Grist, N., Barnett, P., Smart, J.D., 2000. An atomic force microscopy investigation of bioadhesive polymer adsorption onto human buccal cells. *Int. J. Pharm.* 200, 271–277.
 Rossi, S., Sandri, G., Caramella, C.M., 2005. Buccal drug delivery: a challenge already won? *Drug Discov. Today Tech.* 2, 2005.
 Schmidgall, J., Hensel, A., 2002. Bioadhesive properties of polygalacturonides against colonic epithelial membranes. *Int. J. Biol. Macromol.* 30, 217–225.
 Smart, J.D., 2005. The basic and underlying mechanisms of mucoadhesion. *Adv. Drug Deliv. Rev.* 57, 1556–1568.
 Sriamornsak, P., Wattanakorn, N., Takeuchi, H., 2010. Study on the mucoadhesion mechanism of pectin by atomic force microscopy and mucin–particle method. *Carbohydr. Polym.* 79, 54–59.
 Surapaneni, M.S., Das, S.K., Das, N.G., 2006. Effect of excipient and processing variables on adhesive properties and release profile of pentoxifylline from mucoadhesive tablets. *Drug Dev. Ind. Pharm.* 32, 377–387.
 Svensson, O., Lindh, L., Cárdenas, M., Arnebrant, T., 2006. Layer-by-layer assembly of mucin and chitosan–influence of surface properties, concentration and type of mucin. *J. Colloid Interface Sci.* 299, 608–616.
 Takeuchi, H., Thongborisute, J., Matsui, Y., Sugihara, H., Yamamoto, H., Kawashima, Y., 2005. Novel mucoadhesion tests for polymer and polymer-coated particles to design optimal mucoadhesive drug delivery systems. *Adv. Drug Deliv. Rev.* 57, 1583–1594.
 Thirawong, N., Nunthanid, J., Puttipipatkachorn, S., Sriamornsak, P., 2007. Mucoadhesive properties of various pectins on gastrointestinal mucosa: An in vitro evaluation using texture analyzer. *Eur. J. Pharm. Biopharm.* 67, 132–140.
 Thirawong, N., Kennedy, R.A., Sriamornsak, P., 2008. Viscometric study of pectin–mucin interaction and its mucoadhesive bond strength. *Carbohydr. Polym.* 71, 170–179.
 Thongborisute, J., Takeuchi, H., 2008. Evaluation of mucoadhesiveness of polymers by BIACORE method and mucin–particle method. *Int. J. Pharm.* 354, 204–209.